Hernandez-Estrada, Albert; Reza, Mehedi; Hughes, Mark

The structure of dislocations in hemp (Cannabis sativa L.) fibres and implications for mechanical behaviour

Published in:
BioResources

DOI:
10.15376/biores.15.2.2579-2595

Published: 01/05/2020

Document Version
Publisher's PDF, also known as Version of record

Please cite the original version:
Hernandez-Estrada, A., Reza, M., & Hughes, M. (2020). The structure of dislocations in hemp (Cannabis sativa L.) fibres and implications for mechanical behaviour. *BioResources*, *15*(2), 2579-2595. https://doi.org/10.15376/biores.15.2.2579-2595

The Structure of Dislocations in Hemp (*Cannabis sativa* L.) Fibres and Implications for Mechanical Behaviour

Albert Hernandez-Estrada,[a,c,*] Mehedi Reza,[b] and Mark Hughes [a]

Elementary fibres isolated from mechanically processed technical hemp were axially sectioned and imaged with transmission electron microscopy (TEM) to reveal details of the axial morphology of dislocations in the fibre. The overall aim was to investigate the detailed axial structural changes that the fibres undergo during processing, to help better understand the alterations in the deformation behaviour the fibres undergo following processing. The images showed the structure and morphology of dislocations as well as the different forms of damage that processing produced in the fibre structure, such as misalignment of the microfibrils, delamination, and buckled cellulose microfibrils. Furthermore, the results of this work show the ability that axial sectioning of the fibre has to reveal new details of the cell wall structure of hemp to offer new insights in the study of the fibre structure. In turn, the results of this work may help explain the mechanical behaviour of the fibres when they are loaded, as well as help explain the greater chemical accessibility of dislocations, for example, when the fibre is acid hydrolysed.

Keywords: Cannabis sativa L.; Hemp; Fibre; Dislocation; Electron microscopy

*Contact information: a: Aalto University School of Chemical Engineering, Department of Bioproducts and Biosystems, P.O. Box 16300, 00076 Aalto, Finland; b: Aalto University School of Science, Department of Applied Physics, P.O. Box 11100, 00076 Aalto, Finland; c: Leibniz Institute for Agricultural Engineering and Bioeconomy (ATB), Department of Post-Harvest Technology, Max-Eyth-Allee 100, 14469 Potsdam, Germany; *Corresponding author: ahernandez@atb-potsdam.de*

ABBREVIATIONS USED IN THE IMAGES

CS - Carbon support film (film in the carbon-coated transmission electron microscopy grid)
CT - Collapsed tissue (wrinkled tissue region)
D - Delamination
FS - Folded section (over the same section)
GS - Grid support
I - (fibre-resin) Interface
ML - Middle lamella
P - Pore (void space in the fibre structure)

INTRODUCTION

An important aspect of the industrial processing of fibre-bearing crop plants such as flax (*Linum usitatissimum* L.) and hemp (*Cannabis sativa* L.) is the biotechnological and mechanical separation of the technical fibres from the stem so that they can be used in applications like textiles (Amaducci and Gusovius 2010) and as reinforcement in composite materials (Gomina 2012). Technical fibres resulting from processing the stems are collections of elementary (single) fibres attached together forming a bundle (Bos and

Donald 1999; Müssig *et al.* 2010). The fibres have widths in the range of 25 to 500 µm, whereas for the elementary fibres, the fibre width is in the range of 3 to 51 µm (Müssig *et al.* 2010). However, mechanical processing of the stem has a negative impact on the fibre structure, leading to the formation of defects, which are frequently referred to dislocations (Nyholm *et al.* 2001; Thygesen and Ander 2005; Thygesen 2008). Formation of such defects can have an irreversible impact on the mechanical properties of the fibre (Thygesen *et al.* 2011) and composites in which the fibres are used as reinforcement (Hughes 2012). When fibres containing dislocations are used as composite reinforcement, they result in localised stress concentrations (Hughes *et al.* 2000; Eichhorn and Young 2003) that can lead to debonding at the fibre-matrix interface (Hughes *et al.* 2000), thereby compromising the performance of the composite and limiting the potential applications for these materials.

Characteristics of Dislocations in Natural Fibres

Dislocations in natural fibres are misalignments of the cellulose microfibrils located in the structure of the secondary cell wall layer (S_2) (Dinwoodie 1968; Nyholm *et al.* 2001). If severe, the dislocations can deform the entire cell wall structure and, in these situations, they are clearly visible when using low magnification light microscopy (Hughes *et al.* 2000) or scanning electron microscopy (SEM) (Bos and Donald 1999; Baley 2004; Thygesen *et al.* 2006b).

Dislocations are also visible using dark-field polarised light microscopy due to a change in the optical properties of the cell wall resulting from a misalignment of the cellulose microfibrils (*e.g.*, Dinwoodie 1968; Nyholm *et al.* 2001). This characteristic can be used to assess the extent of fibre damage (Thygesen and Ander 2005; Mortensen and Madsen 2014). Another feature of dislocations is that they are more chemically reactive (Akin 2010) than the undamaged part of the fibre, making them susceptible to attack, for example, by acid hydrolysis (Ander *et al.* 2005; Hänninen *et al.* 2012; Hernandez-Estrada *et al.* 2016) or enzymatic hydrolysis (Foulk *et al.* 2008). This characteristic has been used in the quantification of dislocations in natural fibres. By first subjecting the fibres to acid hydrolysis, which induces cleavage of the fibre at the dislocation, and then by further analysing the resulting segmentation (Thygesen 2008; Hernandez-Estrada *et al.* 2016), information about the frequency and severity of the dislocations can be obtained (Hernandez-Estrada *et al.* 2016). Moreover, dislocations also act as mechanically weak points (Baley 2004; Thygesen *et al.* 2014; Castellani *et al.* 2016), and the fibres tend to break near the dislocations when, for example, they are loaded in tension (Baley 2004; Thygesen *et al.* 2007).

Internal Structure of Dislocations

Thygesen and Gierlinger (2013) found that the orientation of the cellulose microfibrils within the dislocations in hemp fibre is different to that of the microfibrils in the un-damaged parts of the fibres. Furthermore, these authors noted that cellulose in the un-damaged zones appears to have a more homogeneous orientation compared to cellulose within the dislocations themselves. Thygesen and Gierlinger (2013) used Raman spectroscopy to analyse the compositions of the dislocated and the un-damaged regions of the cell wall; the results indicated that there were no substantial differences in terms of composition.

Bos and Donald (1999) performed a loop test on flax fibres and observed that plastic deformation starts on the compression side of the fibre; however, failure occurs on the tension side. The results of the loop tests performed by Bos and Donald (1999)

suggested that the secondary cell wall of the fibre, in the region of the dislocation, might have already been damaged before the tests began, despite the primary cell wall being apparently undamaged. Zhang *et al.* (2015) investigated the internal structure of dislocations in flax fibres by removing fibre material using a focused ion beam (FIB) technique and thereafter imaging with SEM. This revealed the presence of void spaces in the internal fibre structure in the area of dislocations that resembled pores, which might explain the observations of Bos and Donald (1999).

Regarding the cell wall structure, Thygesen *et al.* (2007) noted that hemp fibres loaded in tension seem to break by shear failure within the cell wall instead of by tensile failure. Bos *et al.* (2002) found similar inter-cell wall delamination failure when testing flax fibres in a loop configuration. Moreover, the results of Bos *et al.* (2002) shed light on the layered structure of the cell wall in flax fibres, and further investigations suggested their multilayer character (Charlet *et al.* 2010). The SEM and transmission electron microscopy (TEM) observations of hemp fibres reported by Thygesen *et al.* (2006a) showed that the S_2 cell wall layer had a laminate structure formed from 1 to 4 major concentric layers each between 1 and 5 μm in thickness. Each of these individual layers was composed of thinner layers approximately 100 nm in thickness. Further, thin layers that were between 200 and 240 nm in thickness were located between the major concentric layers. Further visualization of the fracture zone confirmed that the thicker layers within the S_2 cell wall layer are weakly attached to each other.

Though much more is now known about the characteristics, structure, and occurrence of these dislocations in natural fibres, understanding of the detailed organisation of the cell wall within the dislocation, and how this differs from the surrounding, undamaged parts of the fibre, is still incomplete. Through a better understanding of the nature of the cell wall structure within the dislocations, it should be possible to devise strategies to minimise their adverse effects in technical applications. In this paper, the authors present the findings of a study into the structure of the cell wall within dislocations formed in hemp fibre during processing. The authors used a method of axially sectioning the fibre along its length to conduct an investigation using TEM, combined with three different maceration and two embedding techniques. The findings from this work are expected to substantially improve the understanding of why, for example, the mechanical properties of processed fibres are reduced and why non-linear behaviour is observed in the stress-strain curves of fibres loaded in axial tension. Another aim was to help understand why dislocations result in localised higher chemical reactivity when compared, for instance, with the un-damaged zones of the fibre.

EXPERIMENTAL

Materials

The hemp (*Cannabis sativa* L.) used in this work was the variety USO-31, grown and harvested manually in 2012 in an experimental plot at the Leibniz Institute for Agricultural Engineering and Bioeconomy (Potsdam, Germany). The hemp stalks were dew-retted, and the straw was separated from the core part of the stem (shives) with a laboratory-scale decorticator (Worthmann Maschinenbau GmbH, Barßel-Harkebrügge, Germany) equipped with four pairs of helically-geared rollers with involute profile and with the upper row of rollers made of polytetrafluoroethylene (PTFE) and the lower row made of steel. After decortication, the straw was refined using a laboratory carding machine

(Shirley Developments Ltd., Stockport, England; 500-mm cylinder circumference) to produce technical fibres, *i.e.*, fibre bundles. Figure 1A shows an image of the processed fibre, and more comprehensive information about the material and fibre processing can be found in Hernandez-Estrada *et al.* (2016). Detailed information about the decorticator can be found in Wang *et al.* (2018).

Fibre maceration

Three methods were used to isolate elementary fibres (single cells) from the technical fibres. Two methods were based on maceration in acetic acid and hydrogen peroxide, a method used in plant histology to separate plant tissue into single cells for further study (*e.g.*, Catling and Grayson 1982; Safdari and Devall 2012), and the third method used water to isolate the elementary fibres from the technical fibres.

Maceration using acetic acid and hydrogen peroxide was accomplished by immersing 0.2 g of technical fibres in a 50-mL glass bottle containing 40 mL of a 1:1 mixture of 100% glacial acetic acid and 20% hydrogen peroxide. The mixture was maintained at 60 °C using an oven for 48 h (method-1), after which the elementary fibres were easily separated. The second maceration (method-2) used the same glacial acetic acid/hydrogen peroxide mixture as method-1, but in this instance the fibres were maintained at room temperature for 6 months. In both methods, after maceration the fibres were cleaned with an abundance of millipore quality water and retained for embedding in resin. The third method (method-3) involved immersing 0.2 g of technical fibres in millipore quality water contained in a 50-mL bottle. The bottle was maintained at 30 °C for 72 h using a water bath. The aim of using this method was to retain the fibre structure (Bourmaud *et al.* 2010) and has been used in previous works, *e.g.*, Placet *et al.* (2014).

Methods

Fibre embedding in resin

The elementary fibres isolated using the three fibre isolation methods were soaked in 0.5% glutaraldehyde (a chemical cross-linker) (Sigma-Aldrich, St. Louis, MO, USA) for 45 min followed by pre-staining with 1% (w/v) $KMnO_4$ (VWR International, Radnor, PA, USA) for 45 min, both conducted at room temperature. These pre-staining methods were needed for TEM microscopy to visualize the fibre and the authors refer the interested reader to Reza *et al.* (2015) for a more comprehensive overview of specimen preparation for TEM.

Elementary hemp fibres were then mounted in 14 mm × 5 mm × 4 mm (Fig. 1C) silicone moulds, and thereafter the fibres were dehydrated *in situ* using an ethanol series. Concentrations of 60%, 70%, 80%, 90%, and 99.5% ethanol in water were used for the dehydration, with the fibres being immersed for 10 min at each concentration. After the final step, in 99.5% ethanol, the fibres were immersed in 100% acetone for 10 min.

Immediately following dehydration, the fibres were embedded in resin, which was completed using AGR1078 low viscosity epoxy resin (Agar Scientific, Stansted, UK). This consisted of four components: resin, two hardeners, and an accelerator; the mixture is hereinafter referred to as "resin". Embedding in resin was accomplished using two different procedures: one aimed at facilitating the penetration of resin into the fibre structure and the other aimed at preventing resin penetration into the fibre structure. Elementary fibres isolated with method-1 and method-3 were placed in a 1:1 mixture of 100% acetone and resin (without accelerator) for 2 h to allow the resin to penetrate the fibre structure. This was followed by embedding in pure resin (with accelerator) and placement under vacuum at -0.1 MPa for 20 min (to facilitate the penetration of resin into the fibre structure).

Elementary fibres prepared using method-2 were directly embedded in resin immediately following the dehydration process without the use of vacuum, to minimize resin penetration into the fibre structure. The silicone moulds with the specimens and the resin were placed in an oven at 60 ºC for 24 h to cure. A schematic overview of the specimen preparation procedure is shown in Fig. 1B to Fig. 1D.

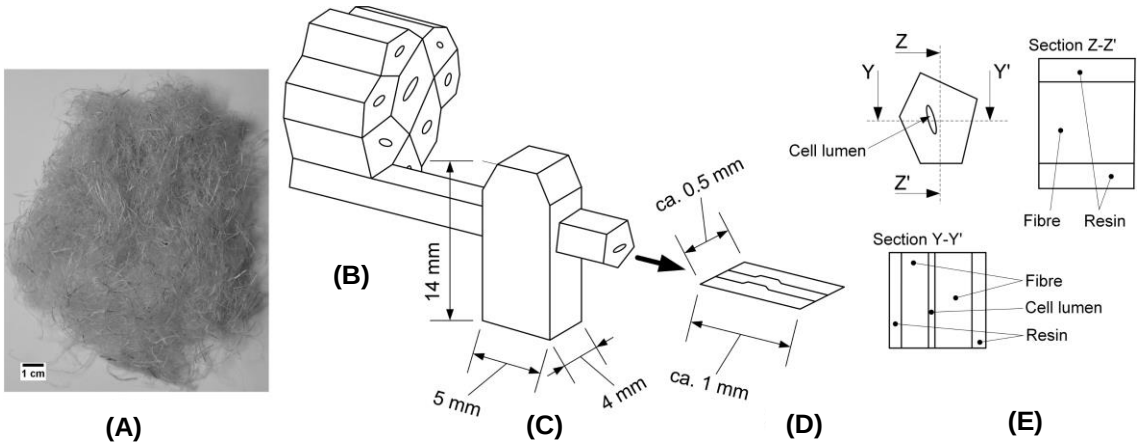

Fig. 1. Specimen preparation method: (A) technical hemp fibre used in this work, (B) Elementary (single cell) fibre isolation from the technical fibre, (C) resin embedding of the elementary fibre, and (D) ultramicrotoming for TEM section preparation; (E) sketch showing two different axial sections that can be obtained from the central part of an elementary fibre sectioning at two different orientations, one including the cell lumen (*i.e.*, Y-Y') and another one not (*i.e.* Z-Z')

Figure 1E shows schematically the effect of sectioning at two different orientations, both cut axially from the central part of the fibre. In one case the section contains the cell lumen and in the other case not (sections Y-Y' and Z-Z', respectively). Because many different sections can be produced from an elementary fibre without certainty of it containing the cell lumen, in some images of this work the presence or not of the cell lumen is an uncertainty that needs to be taken into account, because it can appear as a delamination failure of the fibre.

Sample preparation for TEM

Following curing, excess resin on the blocks containing the fibre specimens was trimmed off using a LEICA EM-TRIM trimming device (Leica Microsystems, Wetzlar, Germany). Thereafter, ultrathin sections of 100 to 150 nm were cut in the longitudinal direction of the fibre in distilled water using a diamond knife on a Leica EM UC7 ultramicrotome (Leica Microsystems, Wetzlar, Germany) at room temperature (see Fig. 1D). One fibre specimen from each preparation method was sectioned. Only sections from the central part of the fibre were used.

Sections were collected on copper grids by gently touching the sections floating in the water bath. Two types of grids were used in this work: one with a carbon support film and one without. These were respectively Lacey carbon films (Electron Microscopy Sciences, Hatfield, PA, USA) and 400-mesh square Cu grids (Agar Scientific Ltd, Stansted, UK), hereinafter referred to as "grid with carbon film" and "grid without carbon film". The authors refer the reader to Reza *et al.* (2015) for more comprehensive and detailed information about specimen preparation for the TEM analysis of natural fibre and wood specimens.

The ultrathin resin-fibre sections were analysed with a Jeol JEM-3200FSC (JEOL Ltd., Akishima, Tokyo, Japan) field-emission cryo-transmission electron microscope at an accelerating voltage of 300 kV. Micrographs were recorded using a Gatan Ultrascan 4000 CCD camera (Gatan, Pleasanton, CA, USA) and using Gatan Digital Micrograph software (Gatan, version 1.83.842, Pleasanton, CA, USA). The imaging was performed using zero-loss energy filtering (Omega type) with a slit width of 20 eV. The specimen temperature was maintained at -187 °C with liquid nitrogen.

RESULTS AND DISCUSSION

The results of this work clearly showed that the dislocations found in technical hemp fibre, induced during processing, resemble those reported previously (*e.g.*, Hughes *et al.* 2000; Thygesen *et al.* 2006b), or that have been observed in flax (Bos and Donald 1999; Bos *et al.* 2002; Zhang *et al.* 2015). Furthermore, the use of different specimen preparation methods proved to be an advantage when trying to reveal different structural features.

Morphology of Dislocations

Figure 2 shows an image from a section of an elementary hemp fibre isolated by maceration using acetic acid and hydrogen peroxide (method-1) and mounted on a grid without carbon film (GS in Fig. 2). The image clearly shows a large dislocation, approximately 30 µm in length. The dislocation appears to have been produced through compression stresses in the longitudinal direction of the fibre, and the morphology is reminiscent of the dislocations published in literature (*e.g.*, Hughes *et al.* 2000; Thygesen *et al.* 2006b).

The dislocation shown in Fig. 2 also exhibits three clearly delineated regions (A, B, and C), with regions A and C resembling each other and region B appearing to show a greater concentration of deformations with different orientations, although a dislocation of this size consists of multiple small and individual dislocations that are more like a complex system. The fibre section in regions A and C is approximately 12 µm in width while in the damaged area (zone B) the fibre width increases to 14 to 15 µm. These results are in agreement with the results of Thygesen and Gierlinger (2013), who observed a dislocation in a hemp fibre using Raman spectroscopy and found more heterogeneous microfibril orientations within the dislocation than in the un-damaged areas surrounding the dislocation.

Zone B in Fig. 2 also appears to show an opening-up of the structure of the fibre resulting in axial delamination (*e.g.*, D1 and D2 in Fig. 2) of the cell wall that could account for the increased width. Outside zone B, delamination did not seem to have occurred extensively, other than what appears to be some minor delamination near to the boundary with zone B (*e.g.*, D3 in Fig. 2). It is perhaps difficult to categorically assert that the features D1 and D2 (Fig. 2) are indeed the result of delamination produced during fibre processing and not the cell lumen, but this seems reasonable given that it appears to be continuous and, moreover, it becomes indistinguishable as it enters zones A and C (in Fig. 2). Nevertheless, the presence or not of the cell lumen in the section is a recurrent feature. This is a matter of uncertainty in the sections produced in this work, as presented in Fig. 1E, and there is a need to take this into account in further analysis.

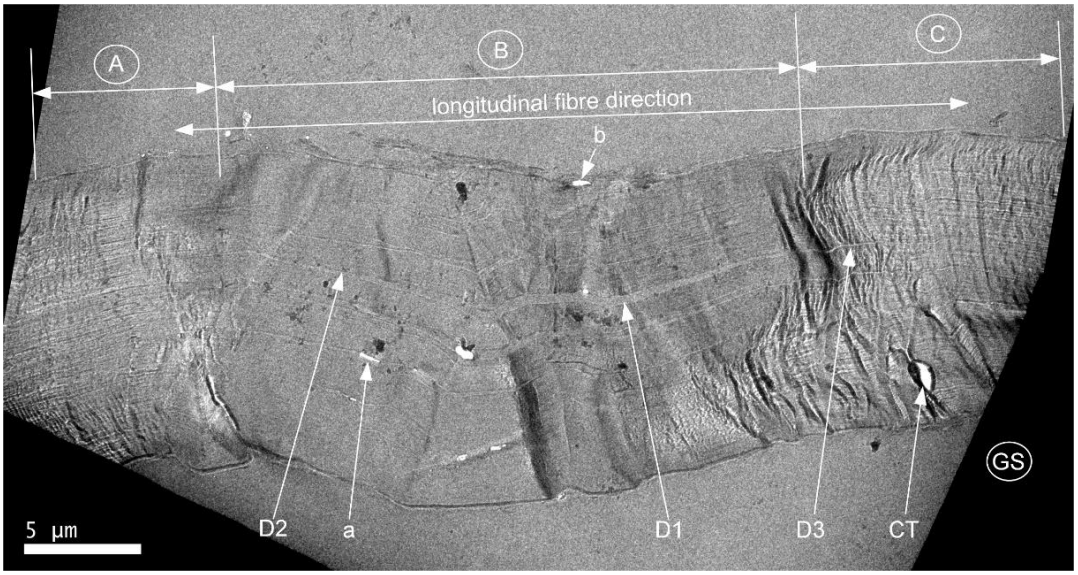

Fig. 2. TEM image of a dislocation in elementary hemp fibre isolated with method-1 and supported on a grid without carbon film

Figure 2 also shows some collapsed tissue (CT) in zones A and C, most probably produced during sectioning with the microtome causing compressive stresses that would exceed the compressive strength of the tissue in the longitudinal direction of the fibre, causing local failure. As shown in Fig. 2, this feature did not occur in most of the damaged area (zone B in Fig. 2), probably because the vacuum-assisted embedding process enabled the void spaces inside the delaminations to be filled (*e.g.*, D1 in Fig. 2), thereby giving support to the structure and avoiding compressive failure of the tissue (CT in Fig. 2). This observation incidentally supports the notion that the penetrability into the fibre in the dislocated areas is easier and helps explain why fibres are cleaved primarily at the dislocations, for example, during acid hydrolysis (Thygesen 2008; Hänninen *et al.* 2012; Hernandez-Estrada *et al.* 2016). However, it was also evident that some areas were not effectively filled and that air gaps inside the fibre and air bubbles in the fibre-resin interface remained (Fig. 2a and b, respectively), which might indicate that a longer vacuum time would be needed for complete penetration.

Figure 3A shows another section of the same dislocation shown in Fig. 2, in this case mounted on a grid with carbon film (CS in Fig. 3), which allowed imaging at higher magnification. Figure 3A clearly shows the same external and internal morphology shown in Fig. 2. From the same section shown in Fig. 3A, two images at higher magnification were taken and are shown in Fig. 3B and Fig. 3C.

Figure 3B shows a magnified image of a region in Fig. 3A, which was a region that underwent compressive stresses in the longitudinal direction of the fibre. As shown, a higher degree of deformation of the microfibrils in the cell wall is visible as well as of the fibre-resin boundary (I in Fig. 3B); these features resembled the observations in flax fibre reported by Baley (2004). Because there is no evidence of microfibril breakage, it is clearly understandable that if this fibre is loaded in tension, the microfibrils will tend to align longitudinally, causing them to disappear under polarised light, as observed by Thygesen *et al.* (2007) and Placet *et al.* (2014). It is also clearly understandable, seeing Fig. 3B, that if a fibre with similar deformations is used as reinforcement in a composite material, the geometry of the dislocation might contribute to the initiation of debonding failure, which

most likely supports the findings of Hughes *et al.* (2000) regarding the behaviour of dislocations in composites.

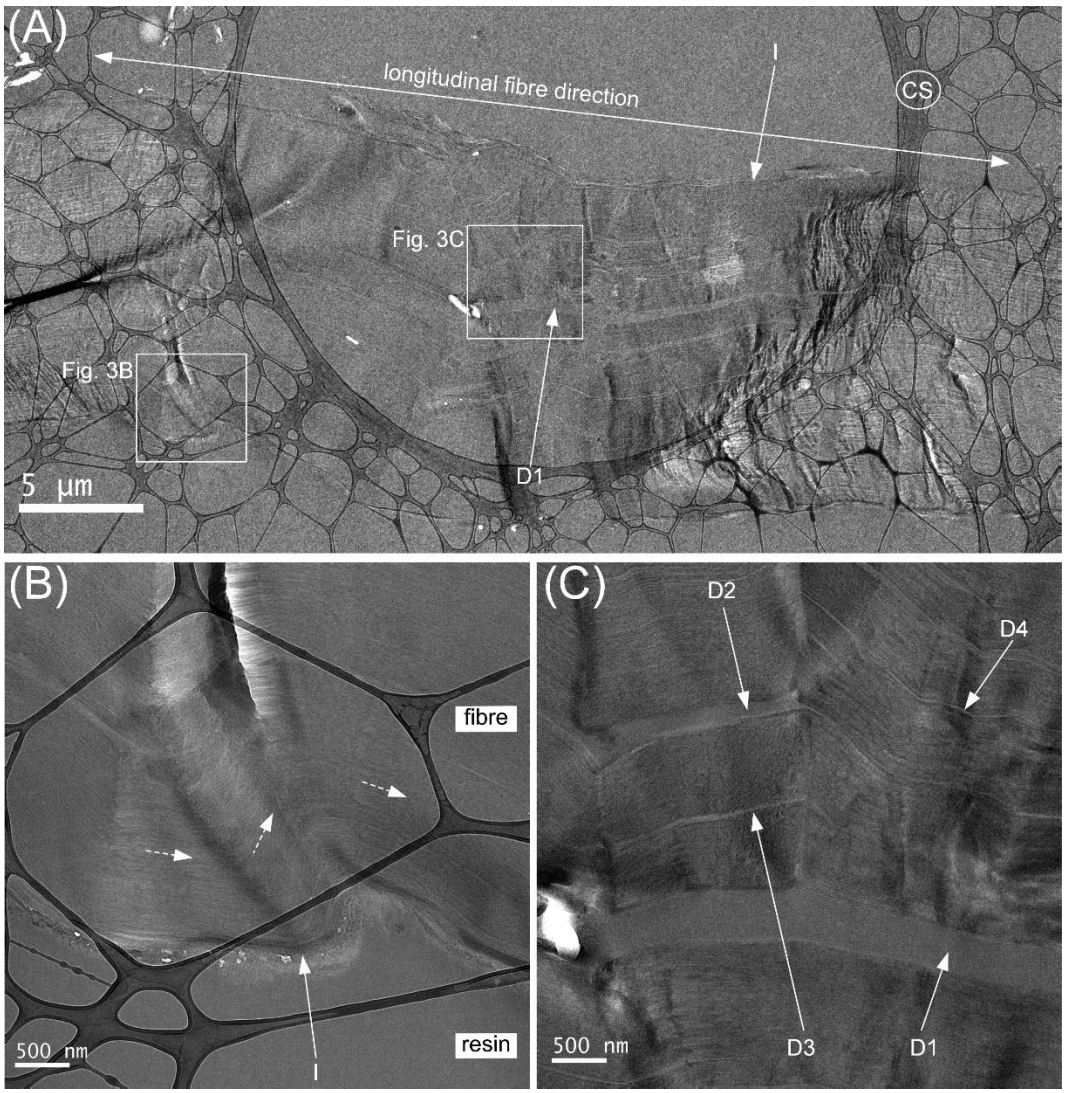

Fig. 3. (A) Dislocation in elementary fibre isolated with method-1 and supported in a grid with carbon film; (B) image at higher magnification of a zone in Fig. 3A, showing the changes in the microfibril orientation within a dislocation in an elementary hemp fibre and on the outer surface (I); and (C) image at higher magnification of a zone in Fig. 3A showing different delaminations and the changes in the microfibril orientation in a dislocation in an elementary hemp fibre

Figure 3C clearly shows the different degrees in delamination failure; for instance, D1 and D2 had larger dimensions than D3 and D4. Moreover, Fig. 3C shows that microfibrils failed in the form of cooperative fibre buckling, which resemble the compression failure of unidirectional fibre-reinforced composites (*e.g.*, Fleck 1997). Furthermore, the narrow feature exemplified by D4 in Fig. 3C could be delamination that occurred between adjacent cell wall sublayers, if the cell wall assumes a multi-layer structure as reported by Thygesen *et al.* (2006a).

Damage Transfer to Adjacent Elementary Fibres

A section from a specimen prepared using method-3 to isolate the elementary fibres and mounted on a grid with carbon film is shown in Fig. 4A. It was noted that method-3, maceration in water, was not as effective at fibre separation compared to maceration in acetic acid and hydrogen peroxide (method-1). This was evident in Fig. 4A, which shows a dislocation approximately 23 µm long and clearly two elementary fibres (F1 and F2 in Fig. 4A) still attached to each other through what it seems to be the middle lamella (ML in Fig. 4A). Figure 4A also shows two delamination failures (D1 and D2 in Fig. 4A) in the region of the dislocation. Elementary fibre F2 (Fig. 4A) had width dimension of approximately 4 to 4.5 µm, whereas the width of the elementary fibre F1 (Fig. 4A) was unknown due to the partially folded section (FS in Fig. 4A). This feature was occasionally observed when sectioning and collecting the sections floating in the water bath with the grid. In some cases, it limited clear visualization of the fibre morphology, as shown in Fig. 4A.

Figure 4B shows, at higher magnification, a detail of the Fig. 4A. As observed, in addition to a noticeable zone of delamination (D3 in Fig. 4B), there was also evidence of smaller delaminations (D4 in Fig. 4B). Figure 4B also shows the existence of what appear to be small areas resembling pores around the delamination D3 (*e.g.*, P1 and P2 in Fig. 4B) that could be damage produced by electron beam irradiation. Electron beam damage is typical in soft materials, and exposing sections to sufficient electron energy can cause damage to the specimen structure (Reza *et al.* 2015). However, the authors used a cryo-TEM, which maintains a temperature of -187 °C during imaging, thus helping to protect the specimens (Reza *et al.* 2015). Furthermore, the authors chose an electron energy suitable for soft materials.

Figure 4C shows at higher magnification, a detail at the fibre-resin interface region in Fig. 4A. In the upper part of the image, there appears to be large deformations in the microfibrillar structure, showing detailed evidence of lighter and darker areas in the fibre parallel to the axis of the fibre, which follows the morphology of the dislocation. This might be related to the findings of Thygesen *et al.* (2006a) who reported the boundary between sublayers of the secondary cell wall layer of hemp fibres being a weak spot in the cell wall structure. Figure 4C also shows that the microfibrils were bent to a greater extent when closer to the outer cell wall layer, which was in general agreement with the dislocation morphology shown in Fig. 3B.

Figure 4D shows a higher magnification image of a delamination failure (D1 in Fig. 4A) that occurred in the vicinity of the middle lamella (ML in Fig. 4A), which in this case was not efficiently filled with resin. Figure 4D shows that some part of fibre F1 still seemed to be effectively attached to the middle lamella (a in Fig. 4D), even though a delamination occurred nearby. The small delamination D5 in Fig. 4E also appeared to have occurred inside the cell wall structure near to, rather than in, the middle lamella (ML in Fig. 4E). This might indicate that within a dislocation, delamination failure between two elementary fibres does not necessarily occur in the middle lamella itself but, rather, inside the cell wall structure, most likely between the primary and secondary cell wall layers. These findings were in agreement with those of Thygesen *et al.* (2006a) who reported that there is weak attachment between the cell wall layers in hemp fibres. This might also help explain the greater accessibility of chemicals into the fibre structure at dislocations reported previously (*e.g.*, Foulk *et al.* 2008; Thygesen 2008; Hänninen *et al.* 2012).

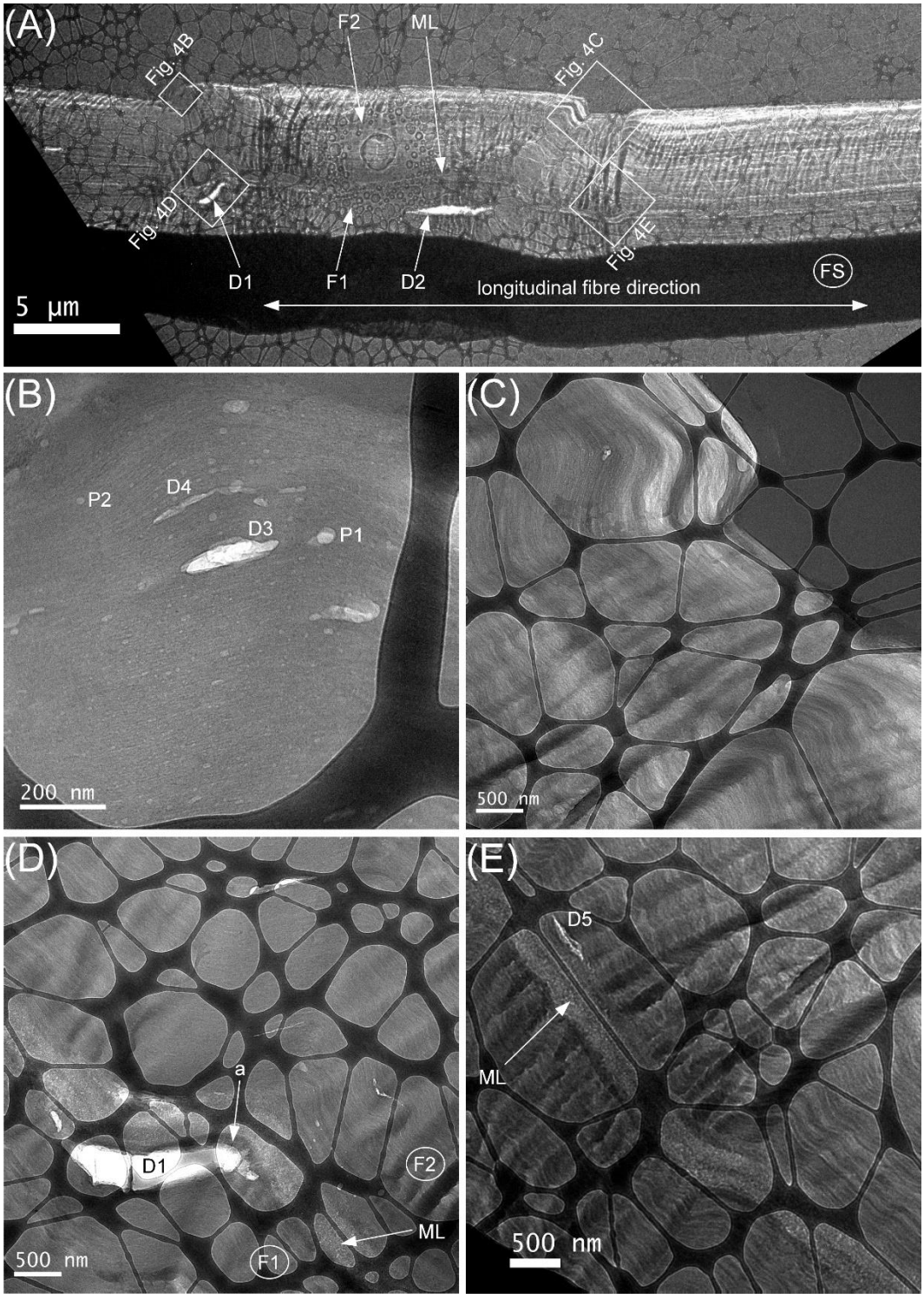

Fig. 4. (A) Dislocation in an elementary hemp fibre isolated using method-3 and mounted in a grid with carbon film, showing what seems to be two elementary fibres (F1 and F2) and the middle lamella (ML). (B) Image at higher magnification of a zone in Fig. 4A showing apparent delaminations and pores (void spaces in the fibre structure related to possible electron beam damage or caused by decortication). (C) Image at higher magnification of a zone in Fig. 4A showing the change of orientation in the microfibril structure. (D) Image at higher magnification of a zone in Fig. 4A showing the delamination D1 close to the ML. (E) Image at higher magnification of a zone in Fig. 4A showing the damage between two elementary hemp fibres.

Ultrastructure of Dislocations

Figure 5 shows a partial dislocation in a section prepared without vacuum (method-3), so as not to favour resin penetration into the fibre structure. At first sight, this technique seemed to have left the fibre tissue unsupported by resin, and it was thus damaged during sectioning. The section clearly shows large zones with collapsed tissue (CT in Fig. 5A) as well as some part of the section folded (FS in Fig. 5A). However, this technique also revealed zones of the fibre structure (zone B in Fig. 5A) that for vacuum-assisted embedding would probably be filled with resin, as shown in Fig. 2 and Fig. 3C.

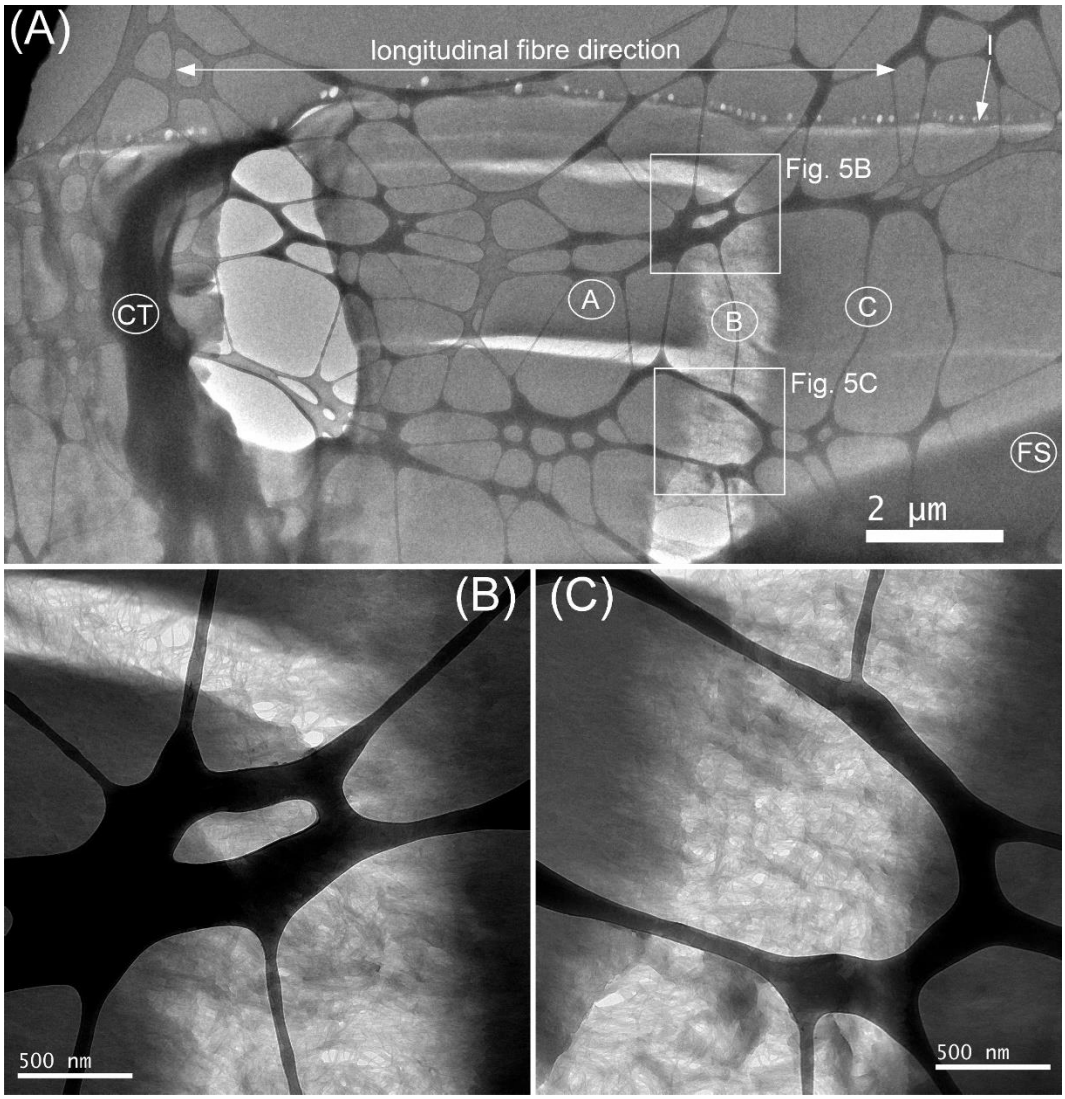

Fig. 5. (A) Dislocation in an elementary hemp fibre isolated using method-2. (B) and (C) Images at higher magnification of zones in Fig. 5A, showing zones with buckled cellulose microfibrils

Figure 5A, for example, shows a zone inside the dislocation where the cellulose microfibrils have buckled entirely (zone B in Fig. 5A). This contrasted with zones in which the cellulose microfibrils were still arranged without apparent disruption (zones A and C in Fig. 5A). Zone B in Fig. 5A suggested a region of weakness in the fibre, wherein failure could be initiated. This helps clarify the observations found in the literature (*e.g.*, Bos *et al.* 2002; Baley 2004) reporting that, for example, flax fibre failure starts in the vicinity of

dislocations when loaded in tension, as well as to studies that report the presence of cellulose aggregates in the fracture zones of fibres tested in tension (*e.g.*, Bos *et al.* 2002; Thygesen *et al.* 2006a). The lighter zone B (Fig. 5A) suggests that during maceration acetic acid might hydrolyse the hemicelluloses, because of the loosened structure, allowing the cellulose microfibrils to be more readily imaged using TEM. It was clear that for vacuum-assisted embedding, this area would most probably be filled with resin which would not allow imaging of the nanofibrils as shown in Figs. 5B and 5C.

Figure 6 shows another section of the same specimen presented in Fig. 5. In this case the dislocation in Fig. 6A appeared less defined and with more collapsed tissue and folded sections (CT and FS, respectively in Fig. 6A). Furthermore, in Fig. 6A and in more detail in Fig. 6B, the presence of void spaces in the fibre structure that look like pores (P1 and P2 in Fig. 6B) was revealed that were not observed in the section shown in Fig. 5.

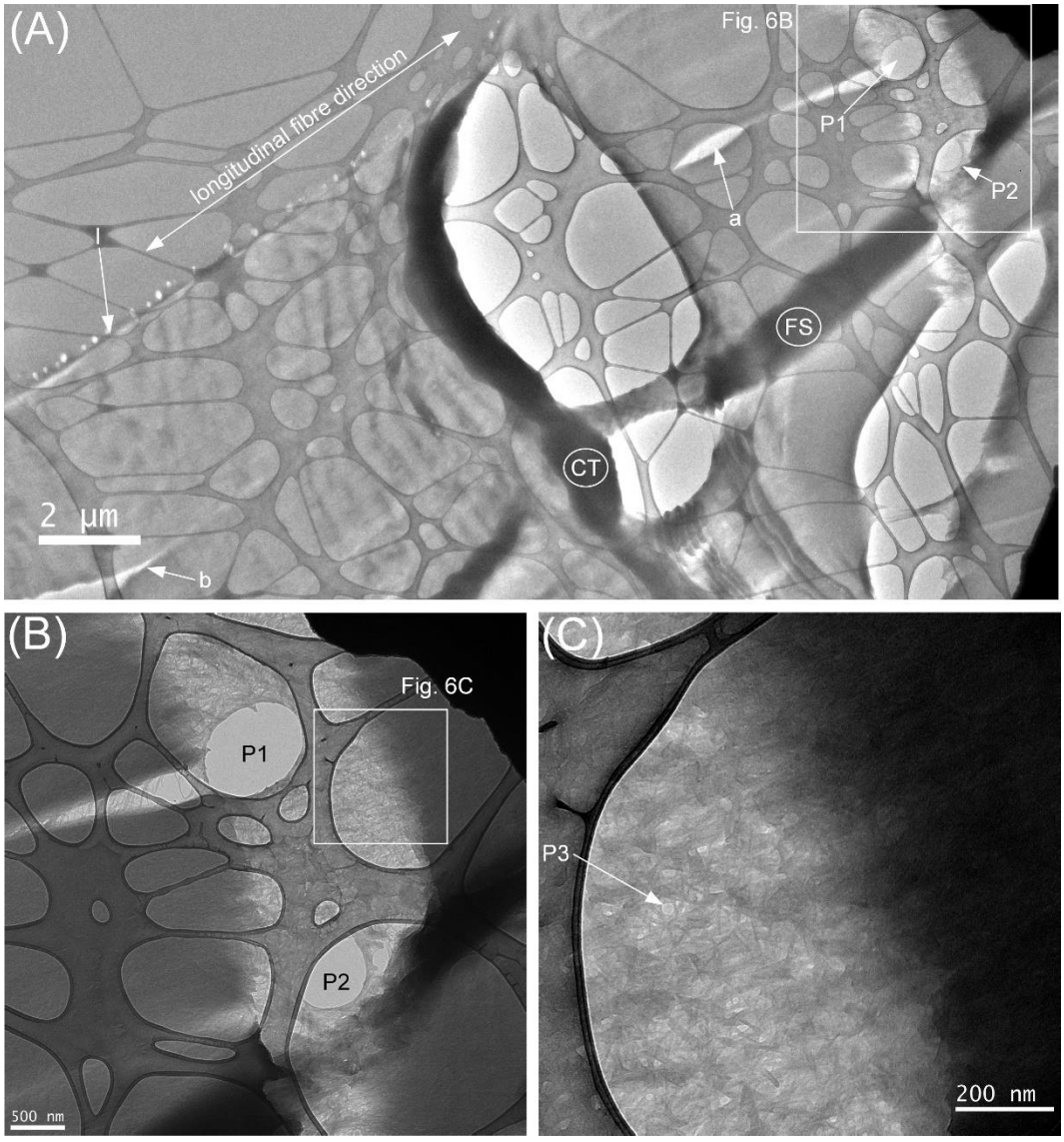

Fig. 6. (A) Dislocation in an elementary hemp fibre isolated using method-2. (A) General image partially showing the zones with buckled cellulose microfibrils. (B) Image at higher magnification of a zone in Fig. 6A showing in detail the void spaces P1 and P2 in the fibre structure). (C) Image at higher magnification of a zone in Fig. 6B showing a zone with buckled cellulose microfibrils.

These void spaces were in the zone where cellulose microfibrils buckled and appear connected to what might be the cell lumen (a in Fig. 6A). The occurrence of these void spaces that look like pores is in agreement with the work published by Zhang *et al.* (2015) who used SEM to visualize the internal structure of a dislocation in flax fibre by removing the fibre material with a FIB. Moreover, in addition to the void spaces P1 and P2 in Fig. 6B, other void spaces were observed (*e.g.*, P3 in Fig. 6C). Figure 6C shows in detail the region with buckled cellulose microfibrils that resemble cellulose nanofibrils (*e.g.*, Pääkkö *et al.* 2007).

Furthermore, the zones with buckled microfibrils might suggest that dislocations produced during the growing of the plant (Thygesen and Asgharipour 2008) might differ from the dislocations produced during processing (*e.g.*, Häninnen *et al.* 2012; Hernandez-Estrada *et al.* 2016). While both features might be misalignments of the cellulose microfibrils, *i.e.*, seen under polarised light as reported in Thygesen and Asgharipour (2008), one would expect that those produced during growth might have a compact structure, *i.e.*, lower accessibility, without the presence of the damage presented in this work (*e.g.*, Fig. 2, Fig. 4A, and Fig. 5). In contrast, damage produced during processing deformed the fibre structure, producing multiple and different damage as shown in Fig. 2 and Fig. 4, which in turn might contribute to increasing the local accessibility at the dislocations. Therefore, it might explain the higher chemical reactivity of the dislocations, for example during acid hydrolysis (Thygesen 2008; Hernandez-Estrada *et al.* 2016), when compared with the non-damaged part of the fibre.

Dislocations and Fibre Mechanical Properties

The fibre deformations shown in Fig. 4A and the evidence of the zones with buckled cellulose microfibrils shown in Fig. 5 help explain the mechanical behaviour of hemp fibres. Firstly, it explains the reduced mechanical properties of processed hemp fibres when compared with fibres that did not undergo mechanical processing (Thygesen *et al.* 2011) as well as the non-linear behaviour observed in the stress-strain curve of natural fibres when loaded axially in tension (Thygesen *et al.* 2007; Duval *et al.* 2011; Placet *et al.* 2014).

At this stage and without more detailed knowledge, it is difficult to categorically assert to what extent the mechanical behaviour is linked to the morphology of dislocations. However, one might expect that, in the initial state of a tensile test in the longitudinal direction of the fibre, a dislocation might look like the one shown in Fig. 2, while after starting the application of tensile loading it would progressively align all the misaligned zones in the dislocation towards the loading direction. This would result in the dislocations disappearing under polarized light microscopy as observed by Thygesen *et al.* (2007) and Placet *et al.* (2014), and somehow it would help explain the non-linear behaviour that the fibre showed when loaded in tension (*e.g.*, Placet *et al.* 2014).

In addition, the buckled microfibrils shown in Fig. 6B facilitated axial alignment of the dislocated zones at the same time as producing strain concentrations around a fibre deformation. However, because the microfibrils were connected to both sides of the un-damaged zones of the fibres (see Fig. 5C), they would be able to carry stress up to a certain point. After the fibre failed at the maximum load, the cellulose microfibrils shown in Fig. 5C would be visible, as noted by Thygesen *et al.* (2006a) and Bos *et al.* (2002).

From the perspective of fibre processing, the results presented in this work may help in the development of alternative processing techniques that could potentially reduce the impact that processing has in the formation of dislocations in natural fibres like hemp

and flax. If such processing developments could be implemented it may lead to improvements in the mechanical properties of composites reinforced with such fibres.

CONCLUSIONS

1. This work showed different morphological characteristics of dislocations in hemp fibres, the feasibility of TEM as a method to study natural materials, and the potential opportunity of axially sectioning the fibre to investigate the dislocation structure.
2. Additionally, the fibre isolation and the specimen preparation methods affected the fibre morphology that was later visualized in TEM.
3. The damage that processing produced in the fibre structure included misorientation of microfibrils, delaminations in the cell wall structure of the fibres, as well as internal zones in the dislocation structure where cellulose microfibrils appeared buckled or contained void spaces in the fibre structure that could be pores.
4. The results contribute to an understanding of the impact of dislocations on the mechanical properties and behaviour of hemp fibres when loaded in tension and how dislocations in flax or hemp fibres might behave when used as reinforcement in composite materials.
5. The results presented in this work help to explain the higher local accessibility at the dislocations, *e.g.*, in acid hydrolysis.

ACKNOWLEDGMENTS

The research leading to these results received funding from the European Union's Seventh Framework Programme FP7-KBBE-2012-6-singlestage (collaborative project) for research, technological development, and demonstration under grant agreement No. 311849 (MultiHemp project - www.multihemp.eu). Albert Hernandez-Estrada wishes to thank the Finnish Cultural Foundation. Kyösti Ruuttunen (Aalto University, Finland) is acknowledged for helpful discussion on natural fibre structure. Jörg Müssig and Birgit Uhrlaub (Bremen University of Applied Sciences, Bremen, Germany) and Hans-Jörg Gusovius and Carsten Lühr (Leibniz Institute for Agricultural Engineering and Bioeconomy, Potsdam, Germany) are thanked for the provision of the processed hemp fibre. This work was carried out at the Aalto University Nanomicroscopy Center (Aalto-NMC).

REFERENCES CITED

Akin, D. E. (2010). "Flax – Structure, chemistry, retting and processing," in: *Industrial Applications of Natural Fibres: Structure, Properties and Technical Applications*, J. Müssig (ed.), John Wiley & Sons, Ltd., Chichester, United Kingdom, pp. 89-108.

Amaducci, S., and Gusovius, H.-J. (2010). "Hemp – Cultivation, extraction and processing," in: *Industrial Applications of Natural Fibres: Structure, Properties and*

Technical Applications, J. Müssig (ed.), John Wiley & Sons, Ltd., Chichester, United Kingdom, pp. 109–134.

Ander, P., Daniel, G., Lindgren, C. G., and Marklund, A. (2005). "Characterization of industrial and laboratory pulp fibres using HCl, cellulase and FiberMaster analysis," *Nordic Pulp & Paper Research Journal* 20(1), 115-121. DOI: 10.3183/npprj-2005-20-01-p115-121

Baley, C. (2004). "Influence of kink bands on the tensile strength of flax fibers," *Journal of Materials Science* 39(1), 331-334. DOI: 10.1023/B:JMSC.0000007768.63055.ae

Bos, H. L., and Donald, A. M. (1999). "*In situ* ESEM study of the deformation of elementary flax fibres," *Journal of Materials Science* 34(13), 3029-3034. DOI: 10.1023/A:1004650126890

Bos, H. L., Van Den Oever, M. J. A., and Peters, O. C. J. J. (2002). "Tensile and compressive properties of flax fibres for natural fibre reinforced composites," *Journal of Materials Science* 37(8), 1683-1692. DOI: 10.1023/A:1014925621252

Bourmaud, A., Morvan, C., and Baley, C. (2010). "Importance of fiber preparation to optimize the surface and mechanical properties of unitary flax fiber," *Industrial Crops and Products* 32(3), 662-667. DOI: 10.1016/j.indcrop.2010.08.002

Castellani, R., Di Giuseppe, E., Beaugrand, J., Dobosz, S., Berzin, F., Vergnes, B., and Budtova, T. (2016). "Lignocellulosic fiber breakage in a molten polymer. Part 1. Qualitative analysis using rheo-optical observations," *Composites Part A: Applied Science and Manufacturing* 91(Part 1), 229-237. DOI: 10.1016/j.compositesa.2016.10.015

Catling, D., and Grayson, J. (1982). *Identification of Vegetable Fibres*, Chapman and Hall, New York, NY, USA.

Charlet, K., Jernot, J. P., Eve, S., Gomina, M., and Bréard, J. (2010). "Multi-scale morphological characterisation of flax: From the stem to the fibrils," *Carbohydrate Polymers* 82(1), 54-61. DOI: 10.1016/j.carbpol.2010.04.022

Dinwoodie, J. M. (1968). "Failure in timber. 1. Microscopic changes in cell-wall structure associated with compression failure," *Journal of the Institute of Wood Science* (21), 37-53.

Duval, A., Bourmaud, A., Augier, L., and Baley, C. (2011). "Influence of the sampling area of the stem on the mechanical properties of hemp fibers," *Materials Letters* 65(4), 797-800. DOI: 10.1016/j.matlet.2010.11.053

Eichhorn, S. J., and Young, R. J. (2003). "Deformation micromechanics of natural cellulose fibre networks and composites," *Composites Science and Technology* 63(9), 1225-1230. DOI: 10.1016/S0266-3538(03)00091-5

Fleck, N. A. (1997). "Compressive failure of fiber composites," in: *Advances in Applied Mechanics*, J. W. Hutchinson, and T. Y. Wu (eds.), Academic Press, Cambridge, MA, USA, pp. 43-117. DOI: 10.1016/S0065-2156(08)70385-5

Foulk, J. A., Akin, D. E., and Dodd, R. B. (2008). "Influence of pectinolytic enzymes on retting effectiveness and resultant fiber properties," *BioResources* 3(1), 155-169. DOI: 10.15376/biores.3.1.155-169

Gomina, M. (2012). "VIII - Flax & hemp composite applications," in: *Flax and Hemp Fibres: A Natural Solution for the Composite Industry*, JEC Composites and CELC, Paris, France, pp. 141–162.

Hänninen, T., Thygesen, A., Mehmood, S., Madsen, B., and Hughes, M. (2012). "Mechanical processing of bast fibres: The occurrence of damage and its effect on

fibre structure," *Industrial Crops and Products* 39, 7-11. DOI: 10.1016/j.indcrop.2012.01.025

Hernandez-Estrada, A., Gusovius, H.-J., Müssig, J., and Hughes, M. (2016). "Assessing the susceptibility of hemp fibre to the formation of dislocations during processing," *Industrial Crops and Products* 85, 382-388. DOI: 10.1016/j.indcrop.2016.01.006

Hughes, M. (2012). "Defects in natural fibres: Their origin, characteristics and implications for natural fibre-reinforced composites," *Journal of Materials Science* 47(2), 599-609. DOI: 10.1007/s10853-011-6025-3

Hughes, M., Sèbe, G., Hague, J., Hill, C., Spear, M., and Mott, L. (2000). "An investigation into the effects of micro-compressive defects on interphase behaviour in hemp-epoxy composites using half-fringe photoelasticity," *Composite Interfaces* 7(1), 13-29. DOI: 10.1163/156855400300183551

Mortensen, U. A., and Madsen, B. (2014). "Protocol for quantification of defects in natural fibres for composites," *Journal of Textiles* 2014, Article ID 929875. DOI: 10.1155/2014/929875

Müssig, J., Fischer, H., Graupner, N., and Drieling, A. (2010). "Testing methods for measuring physical and mechanical fibre properties (plant and animal fibres)," in: *Industrial Applications of Natural Fibres: Structure, Properties and Technical Applications*, J. Müssig (ed.), John Wiley & Sons, Ltd., Chichester, United Kingdom, pp. 269–310.

Nyholm, K., Ander, P., Bardage, S., and Geoffrey, D. (2001). "Dislocations in pulp fibres – their origin, characteristics and importance – A review," *Nordic Pulp & Paper Research Journal* 16(4), 376-384. DOI: 10.3183/npprj-2001-16-04-p376-384

Pääkkö, M., Ankerfors, M., Kosonen, H., Nykänen, A., Ahola, S., Österberg, M., Ruokolainen, J., Laine, J., Larsson, P. T., Ikkala, O., *et al.* (2007). "Enzymatic hydrolysis combined with mechanical shearing and high-pressure homogenization for nanoscale cellulose fibrils and strong gels," *Biomacromolecules* 8(6), 1934-1941. DOI: 10.1021/bm061215p

Placet, V., Cissé, O., and Lamine Boubakar, M. (2014). "Nonlinear tensile behaviour of elementary hemp fibres. Part I: Investigation of the possible origins using repeated progressive loading with in situ microscopic observations," *Composites Part A: Applied Science and Manufacturing* 56, 319-327. DOI: 10.1016/j.compositesa.2012.11.019

Reza, M., Kontturi, E., Jääskeläinen, A.-S., Vuorinen, T., and Ruokolainen, J. (2015). "Transmission electron microscopy for wood and fiber analysis − A review," *BioResources* 10(3), 6230-6261. DOI: 10.15376/biores.10.3.

Safdari, V., and Devall, M. S. (2012). "Identification of important Iranian hardwoods by vessel-ray pits and vessel element shapes (maceration process)," *Lignocellulose* 1(1), 55-70.

Thygesen, L. G., and Ander, P. (2005). "Quantification of dislocations in spruce pulp and hemp fibres using polarized light microscopy and image analysis," *Nordic Pulp & Paper Research Journal* 20(1), 64-71. DOI: 10.3183/npprj-2005-20-01-p064-071

Thygesen, A., Daniel, G., Lilholt, H., and Thomsen, A. B. (2006a). "Hemp fiber microstructure and use of fungal defibration to obtain fibers for composite materials," *Journal of Natural Fibers* 2(4), 19-37. DOI: 10.1300/J395v02n04_02

Thygesen, L. G., Bilde-Sørensen, J. B., and Hoffmeyer, P. (2006b). "Visualisation of dislocations in hemp fibres: A comparison between scanning electron microscopy

(SEM) and polarized light microscopy (PLM)," *Industrial Crops and Products* 24(2), 181-185. DOI: 10.1016/j.indcrop.2006.03.009

Thygesen, L. G., Eder, M., and Burgert, I. (2007). "Dislocations in single hemp fibres—investigations into the relationship of structural distortions and tensile properties at the cell wall level," *Journal of Materials Science* 42(2), 558-564. DOI: 10.1007/s10853-006-1113-5

Thygesen, L. G. (2008). "Quantification of dislocations in hemp fibers using acid hydrolysis and fiber segment length distributions," *Journal of Materials Science* 43(4), 1311-1317. DOI: 10.1007/s10853-007-2284-4

Thygesen, L. G., and Asgharipour, M. R. (2008). "The effects of growth and storage conditions on dislocations in hemp fibres," *Journal of Materials Science* 43(10), 3670-3673. DOI: 10.1007/s10853-008-2587-0

Thygesen, A., Madsen, B., Bjerre, A. B., and Lilholt, H. (2011). "Cellulosic fibers: Effect of processing on fiber bundle strength," *Journal of Natural Fibers* 8(3), 161-175. DOI: 10.1080/15440478.2011.602236

Thygesen, L. G., and Gierlinger, N. (2013). "The molecular structure within dislocations in *Cannabis sativa* fibres studied by polarised Raman microspectroscopy," *Journal of Structural Biology* 182(3), 219-225. DOI: 10.1016/j.jsb.2013.03.010

Thygesen, L. G., Thybring, E. E., Johansen, K. S., and Felby, C. (2014). "The mechanisms of plant cell wall deconstruction during enzymatic hydrolysis," *PLoS ONE* 9(9), e108313. DOI: 10.1371/journal.pone.0108313

Wang, S., Gusovius, H.-J., Lühr, C., Musio, S., Uhrlaub, B., Amaducci, S., and Müssig, J. (2018). "Assessment system to characterise and compare different hemp varieties based on a developed lab-scaled decortication system," *Industrial Crops and Products* 117, 159-168. DOI: 10.1016/j.indcrop.2018.02.083

Zhang, H., Sui, T., Thygesen, L. G., O'Brien, P., and Korsunsky, A. M. (2015). "Multi-modal microscopy characterisation of nodal markings in flax fibre," in: *Proceedings of the World Congress on Engineering 2015 Vol II*, London, England, pp. 1011–1015.

Article submitted: October 13, 2019; Peer review completed: January 23, 2020; Revised version received and accepted: February 16, 2020; Published: February 21, 2020.
DOI: 10.15376/biores.15.2.2579-2595